

## 1.3 THERMAL EFFECTS ON DISPERSION ABOUT STRUCTURES

Sue Ellen Haupt \*  
L. Joel Peltier  
James J. Dreyer  
Robert F. Kunz

Applied Research Laboratory, The Pennsylvania State University, State College, PA

### 1. INTRODUCTION

Many groups have been modeling the dispersion of a contaminant in an urban setting. Such modeling efforts have ranged from using basic dispersion models such as modified plume and puff models (Warner, et al. 2004; Chang, et al. 2005; Haan, et al. 2001) to using full computational fluid dynamics (CFD) models (He, et al. 1997; Thilmany 2005; Leung, et al. 2005; Baik, et al. 2003, Pullen, et al. 2005). Most of those studies have concentrated on the impact to the flow of the physical presence of the buildings. It has been shown that flow, and the resulting dispersion of an effluent, is modified in the building wake (Cowan, et al. 1997; Moon, et al. 1997; Palmer, et al. 2003). It is widely recognized that thermal effects due to the urban heat island can influence flow about a city (Britter and Hanna 2003). What has not been studied yet in full detail is the impact of thermal heating on the flow and effluent dispersion about individual buildings. In particular, some open questions include the impact of time of day, building materials, sky cover, etc. that impact the local thermal heating of a building. All these features effect the buoyancy, and thus, the resulting flow and dispersion about a building.

Yamada (2005) has recently shown temperature variations between urban and rural areas in a CFD model that includes thermal energy balances. Huang, et al. (2005) developed a numerical simulation program incorporating convection, radiation, and conduction including a three dimensional CFD model. They modeled the influence of heat

released from rooftops and conjectured about the resulting influence on atmospheric dispersion.

The purpose of this work is to study the impact of heat transfer – radiation, conduction, and convection – on the dispersion of a contaminant about a building. The problem chosen is a building design that was previously modeled using fine scale CFD for the purposes of choosing appropriate design features (Peltier, et al. 2005).

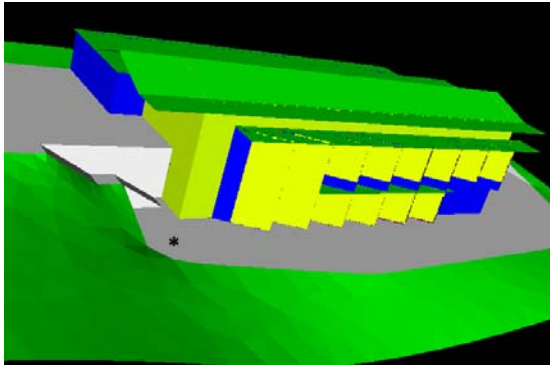
### 2. MODELING APPROACH

#### 2.1 The building

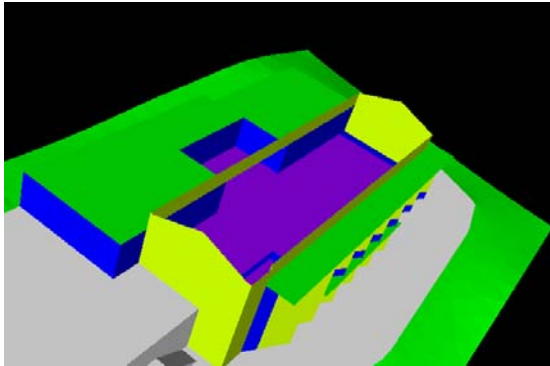
The example building for computing dispersion impact is an environmentally-friendly building design where CFD was used as a design tool. The building design is shown in Figure 1. Figure 1a shows a front view while 1b and 1c look into the upper and lower levels of the building respectively. The building emphasizes passive solar features, including Trombe walls for heat transfer. Those walls are glass on the exterior with a six inch space in front of a masonry wall that receives solar heating. Solar radiation acts to heat the wall, which transfers its heat to the air between the glass and the back wall. As the warmer air rises and is vented into the building, it is replaced by cooler air from below via three air ducts on the interior of the wall. This passive solar heating, as well as the large glass front windows, reduces the need for mechanical heating in winter. The long awnings, however, prevent excessive summer heating when the zenith angle is higher.

---

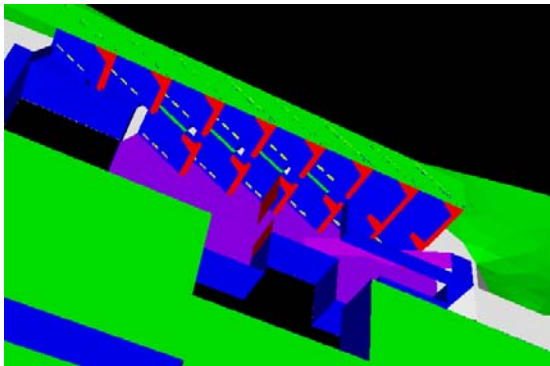
Corresponding author address: Sue Ellen Haupt, Applied Research Laboratory, P.O. Box 30, Pennsylvania State University, State College, PA16804; e-mail: [haupts2@asme.org](mailto:haupts2@asme.org)



a.



b.



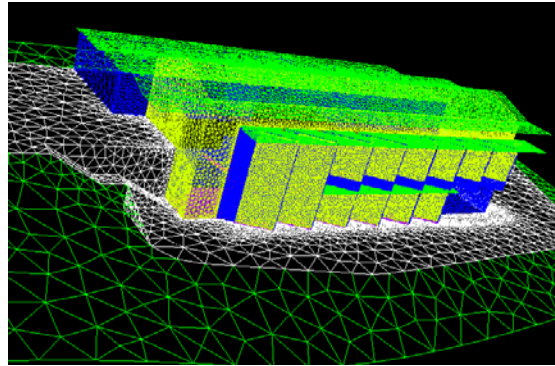
c.

**Figure 1.** Geometry of the building modeled. a. exterior view indicating Trombe walls, b. view of upper level from above with roof removed, and c. view of lower level and inside view of Trombe walls.

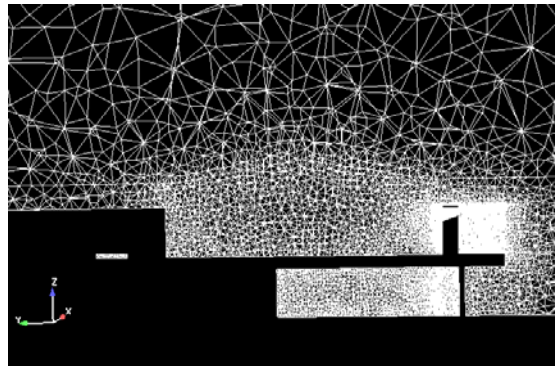
## 2.2 The Mesh

A modeling grid was built around the building and over the terrain using the gridding tool, GRIDGEN. The near wall spacing is 0.15 to 0.5. A finer mesh resolves near wall features close to the building, but this resolution is relaxed further from the walls. A total of over 2.1 million unstructured hexahedral elements

(427,000 grid points) are included in the mesh. The mesh appears in Figure 2. Figure 2a shows the surface mesh over the building and terrain and 2b is a cut plane of the mesh taken through the building. Note the high density of the mesh in the vicinity of the Trombe walls where a significant thermal circulation is expected to develop.



a.



b.

**Figure 2. Building mesh.** a. Exterior mesh indicating finer grid spacing close to building. b. mesh inside building is finer, especially in the small spaces of the Trombe walls.

## 2.3 The CFD Model

The code used in the present work, NPHASE, is three-dimensional, unstructured, parallel, and supports an arbitrary number of constituents. The algorithm follows a segregated pressure based methodology. A collocated variable arrangement is used and a lagged coefficient linearization is applied. One of several diagonal dominance preserving, face-based finite volume spatial discretization schemes is selected for the momentum, volume fraction, interfacial area density and turbulence transport equations. Mixture volume continuity is

introduced through a pressure correction equation, based on the SIMPLE-C algorithm (Van Doormal and Raithby 1984). At each iteration, the discrete momentum equations are solved approximately, followed by a more exact solution of the pressure correction equation. Turbulence scalar, volume fraction and interfacial area density equations are then solved in succession.

Several algorithmic elements critical to the accuracy and robustness of two-fluid simulations with significant inter-field transfer are incorporated. These include:

- inter-field coupling of drag and mass transfer terms within the preconditioning, linear solver and artificial dissipation elements of the scheme,
- appropriate discretization of lift and dispersion forces to prevent odd-even decoupling in the solution,
- formulation of virtual mass as a convection operator.

These features are critical to our future plans to explicitly introduce a second constituent representing an air contaminant.

Standard inflow, symmetry, wall and outflow boundary conditions are employed. Further details on the code and numerics are available in Kunz et. al (2000, 2001).

A high Reynolds number  $k-\varepsilon$  turbulence model is applied for the gaseous field:

$$\frac{\partial}{\partial x_j} (\alpha \rho u_j k) = \frac{\partial}{\partial x_j} \left[ \alpha \left( \mu + \frac{\mu_t}{\sigma_k} \right) \frac{\partial k}{\partial x_j} \right] + P - \alpha \rho \varepsilon + S_k$$

$$\frac{\partial}{\partial x_j} (\alpha \rho u_j \varepsilon) = \frac{\partial}{\partial x_j} \left[ \alpha \left( \mu + \frac{\mu_t}{\sigma_\varepsilon} \right) \frac{\partial \varepsilon}{\partial x_j} \right] + C_1 \frac{\varepsilon}{k} P -$$

$$C_2 \frac{\varepsilon}{k} \alpha \rho \varepsilon + S_\varepsilon$$

where  $\alpha$  = volume fraction

$\rho$  = density

$x_i$  = Cartesian coordinates

$u_i$  = Cartesian velocity

$k$  = turbulent kinetic energy

$\varepsilon$  = turbulence dissipation rate

$\mu$  = molecular viscosity

$\mu_T$  = turbulent viscosity

$P$  = turbulence energy production

$\sigma_k, \sigma_\varepsilon$  = turbulent Prandtl numbers

$C_1, C_2$  = turbulence model constants

$S_k, S_\varepsilon$  are available source/sink terms to extract turbulence energy associated with breakup (Meng and Uhlman 1998; Kunz, et. al. 2003) and to reduce production.

## 2.4 The Heat Transfer Model

The conduction, radiation, and convection portion of the coupled model is provided by the heat transfer simulation tool, RadTherm (Thermoanalytics 2005). RadTherm carries out a full transient thermal analysis including the effects of conduction, radiation, and convection. Conduction heat transfer is primarily dependent on material properties and geometric thickness. The radiation depends on surface properties and view factors, but Radtherm also includes extensive utilities for modeling environmental factors including the effects of:

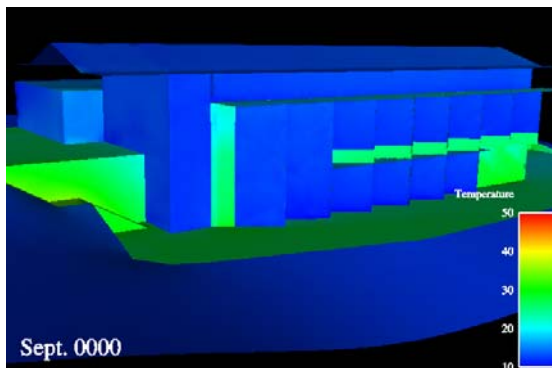
- solar radiation as a function of the position of sun and atmospheric conditions provided by an external weather file,
- full shadowing based on time of day, geometry, and reflections,
- re-radiation between geometric features,
- glass regions that are transparent to solar radiation but opaque to infrared radiation,
- sky radiation.

RadTherm uses ray tracing to compute radiation view factors and solar projected (apparent) areas. The convective heat transfer is modeled in RadTherm using heat transfer coefficients and film temperatures. These parameters are provided by the coupled CFD model NPHASE.

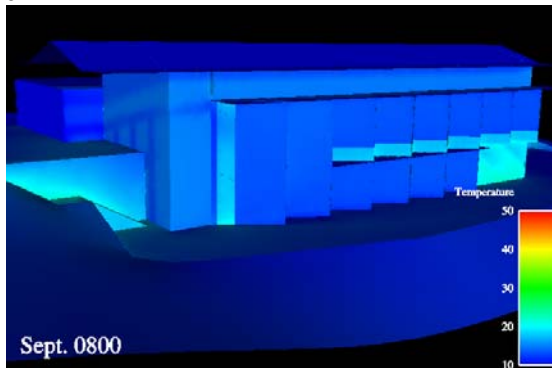
## 2.5 Environmental Conditions

Three separate days of the year are modeled. Complete diurnal cycles are run for a representative warm summer day, a cold winter day, and a day in early autumn. Sunny days were chosen to model the maximum impact of the time-dependent solar radiation forcing function. Within RadTherm, the character of the incident solar energy is determined by the total solar energy flux, the altitude above sea level, the relative humidity, the amount of cloud cover, and the global position and orientation of the building. The latter are fixed geometric properties of the

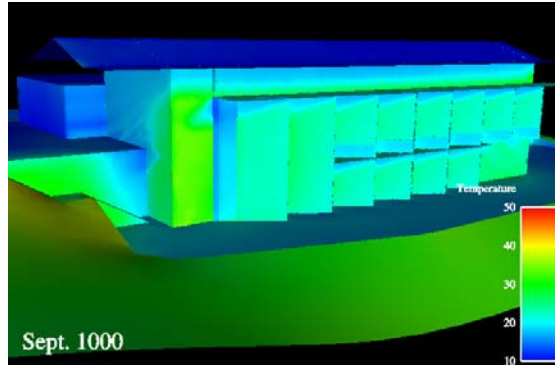
structure that primarily determine the directivity of the radiation and shadowing. Total solar energy flux, relative humidity, and cloud cover are time-dependent weather metrics that are provided by an external weather data file. The source of the weather data used in RadTherm for the diurnal thermal analyses is the Typical Meteorological Year (TMY2) dataset produced by the Analytic Studies Division of the National Renewable Energy Laboratory (NREL 2005). Figure 3 shows how the solar radiation impacts temperatures on the exterior building walls for the September (early autumn) day. Much of the building is cool during the night hours except for around the patio and some areas of the Trombe walls that have retained some heat from the prior day's heating. Radiative heating from the sun becomes evident by 0800 and progresses at 1000. Figure 3d shows the shadowing effects that occur mid-day on the Trombe walls by the overhanging awnings. The patio and walls have heated by mid-afternoon and begin to cool by 1800 as indicated in figure 3f. Low external wind speeds are used (1m/s) to minimize forced convection effects and maximize the free convection buoyancy effects on the heating and cooling of the building.



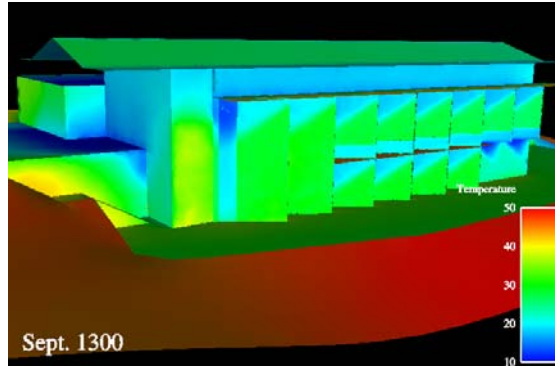
a.



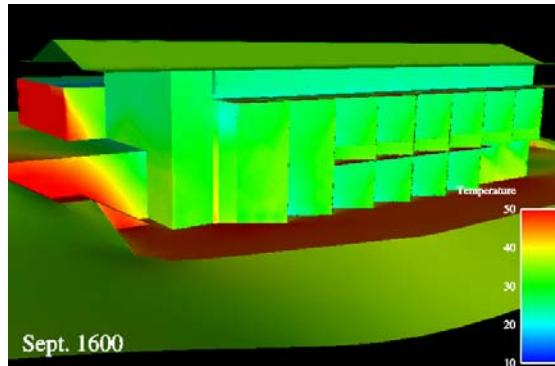
b.



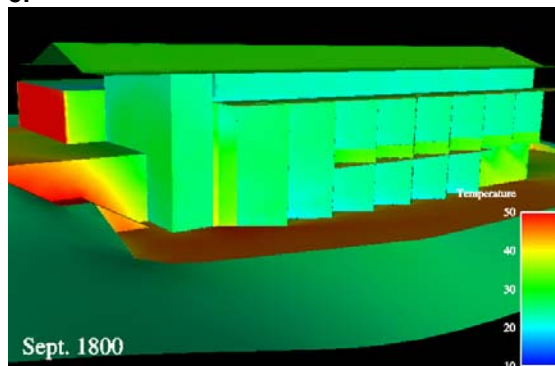
c.



d.



e.



f.

**Figure 3. Temperature cycle on the exterior walls of the building at 6 times of day for the September case: a. 0000, b. 0800, c. 1000, d. 1300, e. 1600, and f. 1800.**

## 2.6 Iterative Solution

A complete diurnal simulation of the heating and cooling of the structure coupled with the (primarily) thermally-driven fluid flow inside and outside the structure is obtained by loosely coupling RADTHERM and NPHASE. The coupling mechanism is as follows: The flow field is updated six times throughout a 24 hour period using steady-state flow solutions computed by NPHASE using instantaneous wall temperatures provided by RADTHERM. The six times are chosen to best represent the most transient portions of the day, e.g., early morning and late afternoon. RADTHERM is then run through a complete 24 hour cycle using convective heat transfer coefficients and fluid film (near wall) temperatures interpolated from the six NPHASE steady solutions in addition to the time-dependent environmental forcing provided by the weather file and the material and surface properties of the building elements. This diurnal analysis is repeated until two consecutive diurnal cycles are effectively indistinguishable, e.g., wall temperatures within  $\sim 1^\circ\text{C}$  within RADTHERM and building internal air temperatures at 1m above the floor as modeled in NPHASE have converged to the same tolerance. This typically requires between 5 and 10 cycles. It is this steady state solution at each of the six times for each of the three cases that is analyzed for differences in the flow field that would be expected to impact dispersion.

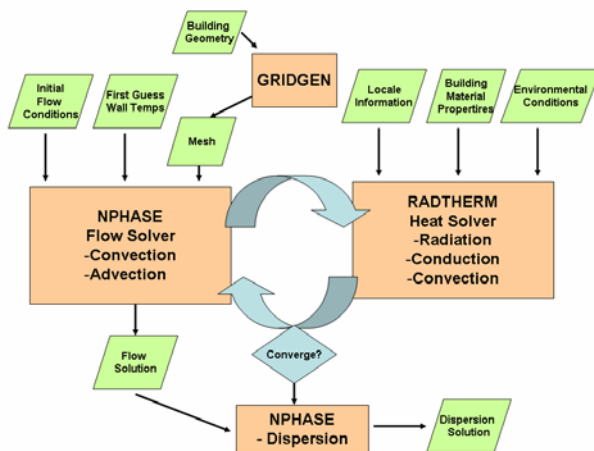


**Figure 4. Flowchart of iterative heat transfer and flow solutions for dispersion.**

Figure 5 shows how the solar angle, when taken together with the building geometry, can result in heating of an internal wall, which results in an elevated wall temperature at that time of day.

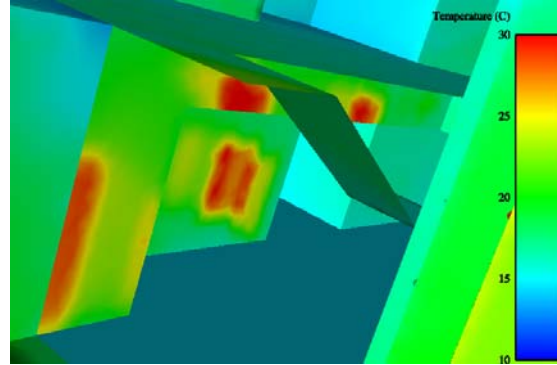


**Figure 5. A view inside the lower level at 1000 for the September case. Heating on the back walls through the windows is evident.**

## 3. RESULTS

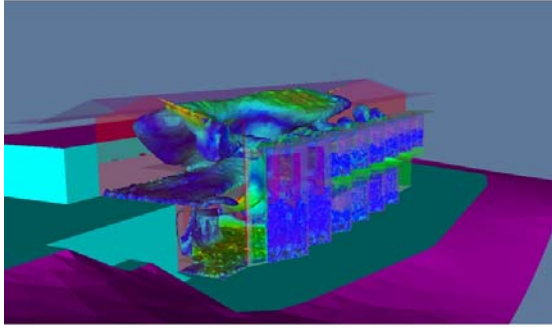
### 3.1 Interior Flow

Dispersion of a neutrally buoyant airborne material will follow the pathlines. Therefore, it is instructive to analyze the small scale flow fields due shear and buoyancy. Full three dimension CFD was accomplished both inside and outside the building with full heating for the December case. Figure 6 shows an isosurface of the temperature field inside the building. The coloring is by velocity magnitude to enable visualization. As expected, the warmer air rises through the open spaces and settles in under the ceiling on the lower level and the roof on the upper level.

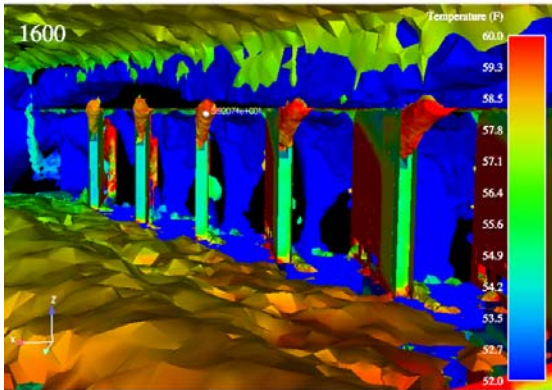
A more detailed look at the interior near the Trombe walls appears in Figure 7. It is apparent that warm air is vented out of the top of the Trombe walls. The heating from the floor is also evident in warmer temperatures near the floor as well as in the air from the Trombe walls.

Figure 8 more closely examines the flow inside the Trombe walls through vector plots. It is obvious that warm air circulates upward both inside and outside the building. The Trombe walls appropriately vent the warmed air into the

building, creating a slow interior buoyancy induced circulation zone.



**Figure 6. Isosurface of temperature colored by velocity magnitude for December heating case at 1600.**



**Figure 7. Inside of building looking at Trombe walls for December case at 1600. Isosurface of velocity magnitude is colored by temperature.**

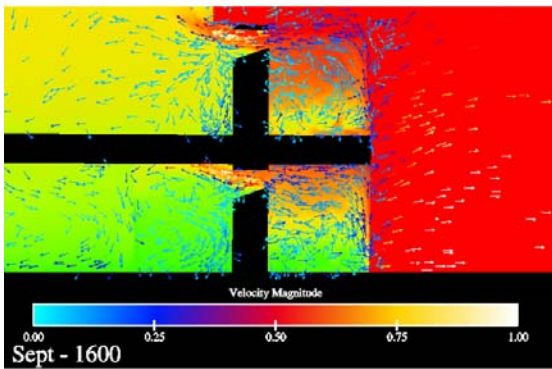
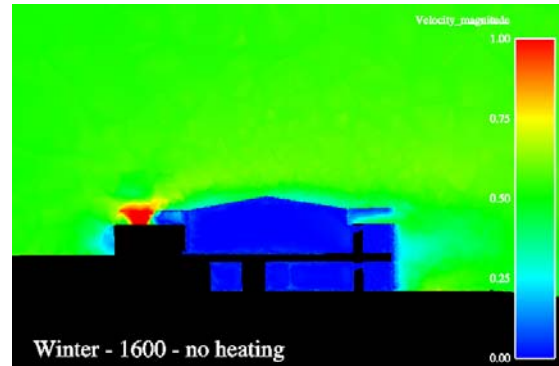


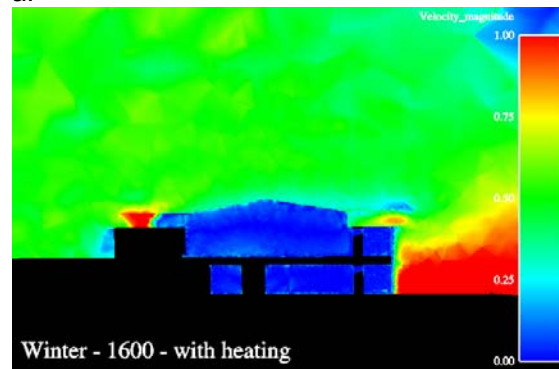
**Figure 8. Velocity vectors near Trombe walls for September case at 1600.**

### 3.2 Exterior Flow

The flow field on the exterior of the building is also modified by the heating. Figure 9 is a clip plane through the building perpendicular to the external wind field. It is colored by velocity magnitude for both the unheated (a) and heated (b) cases at 1600 for the winter day. The left portion of the figures, along the unheated storage section of the building show quite similar velocity plots, as expected, since no differential heating occurs there. The right side, however, is highly affected by the heating due to the Trombe walls. When one breaks the velocity into its components, it is apparent that the change in the x-velocity (parallel to the Trombe walls) is the largest contributor to the differences. This observation is further elucidated by looking down onto a clip plane 5m above the surface in Figure 10. The unheated case (a) shows much slower velocities than the heated version (b).

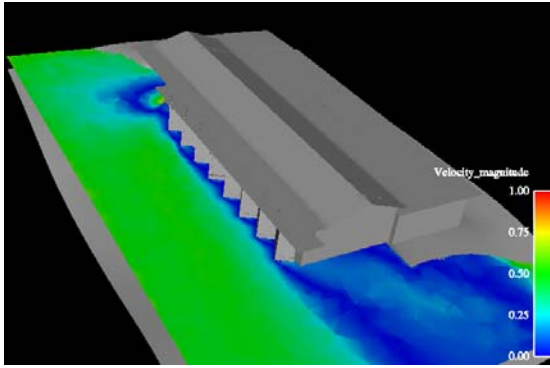


a.

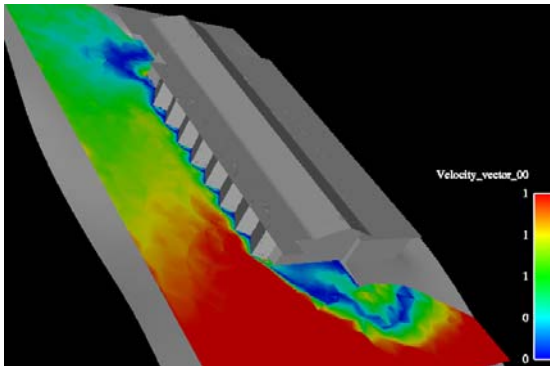


b.

**Figure 9. Clip plane through the building colored by velocity magnitude. a. without heating, and b. with heating at 1600 for the winter case.**



a.

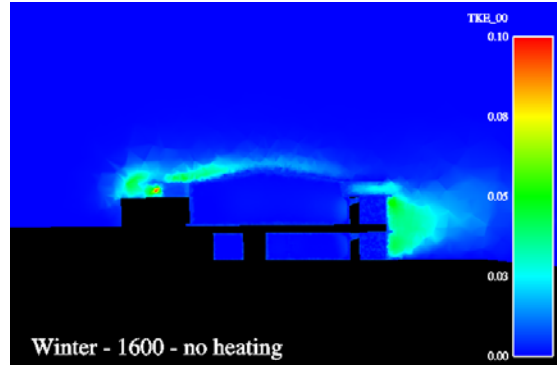


b.

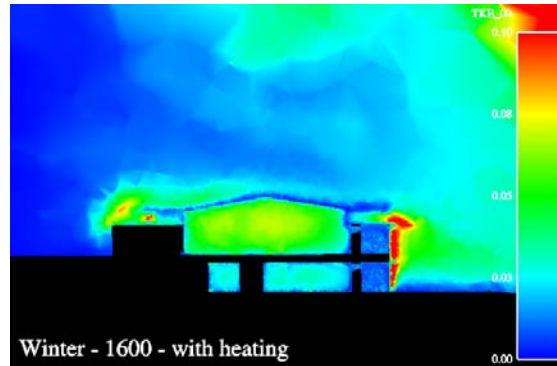
**Figure 10.** Clip plane 5m above surface colored by velocity magnitude. a. without heating, b. winter case with heating at 1600.

The along-building differences are primarily due to the x-velocity, but the differences behind the building were evident in plots of the z-velocity (not shown) where there is a strong downwelling in the lee of the building.

Figure 11 shows differences in the turbulent kinetic energy (TKE, which is computed as  $TKE = (\overline{u^2} + \overline{v^2} + \overline{w^2})/2$ ) for the same winter case. TKE is an indicator of where dispersion differences may come into play. We can see large differences in TKE both along the Trombe walls on the right side of the plots as expected, since that is the location of maximum heating, and also along the left side of the figures in the vicinity of the long awnings. In addition, one can also see enhanced TKE over the roof and in the farfield above the building. When taken together with the wind fields, one would expect dispersion to be enhanced upward and along the Trombe walls and over the roof of the building. In the lee of the building, however, there may be significant subsidence, which would impact the path of potential pollutants.



a.



b.

**Figure 11.** Clip plane showing turbulent kinetic energy for a. no heating, and b. with heating for the December 1600 case.

#### 4. DISCUSSION

Here, we have modeled flow features due to thermal heating using CFD plus models of convection, conduction, and radiation heat transfer employing information on material properties, time of day, shadowing, appropriate models of transparent surfaces, inclusion of sky radiation. What difference do these features make for flow and dispersion within and external to a building?

We have studied three different solar heating cases and compared them to a case with no heat transfer. Internal circulation is widely effected by heating, particularly around the Trombe walls, which demonstrates a significant buoyancy induced circulation. The external circulation shows some impact due to heating. All cases assumed a small external wind speed of 1m/s. There is somewhat more convection from the roof and around the Trombe walls in heated cases, particularly in winter when differential heating is more distinct.

This work is very preliminary. We expect to explicitly model contaminant dispersion both with and without heating in the near. It is a single case study on an isolated building. Although it will give an indication of the impact of heating induced buoyancy on contaminant dispersion, it is still only an example of a single building. It does, however, give us an indication that including heat transfer is expected to modify the fine scale structure of flow about a building. Other buildings could produce somewhat different results. An array of buildings could show different characteristics. We believe further work in this direction is merited to investigate the impact of heating on dispersion in urban areas.

**ACKNOWLEDGEMENTS** –The authors thank Joshua Gassman and Vikram Sami of Lord, Aeck, and Sargent Architecture and John Shaw of Newcomb and Boyd Consultants and Engineers. The paper is inspired by work originally funded by Lord, Aeck, and Sargent Architecture. Part of the work was funded by ARL internal research and development funds.

## REFERENCES

- Baik, J.-J., J.-J. Kim, and H.J.S. Fernando, 2003: A CFD model for simulating urban flow and dispersion, *J. Applied Meteorol.*, **42**, 1636-1648.
- Britter, R.E. and S. R. Hanna, 2003: Flow and dispersion in Urban Areas. *Annu. Rev. Fluid Mech*, **35**, 469-496.
- Chang, J.C., S.R. Hanna, Z. Boybeyi, and P. Franzese, 2005: Use of Salt Lake City URBAN 2000 Field to evaluate the urban hazard prediction assessment capability (HPAC) dispersion model, *J. Applied Meteorol.*, **44**, 485-501.
- Cowan, I.R., I.P. Castro, A.G. Robins, 1997: Numerical considerations for simulations of flow and dispersion around buildings, *J. Wind Eng. & Ind. Aerodynam*, **67/68**, 535-545.
- Haan, P.d., M.W. Rotach, and J. Werfeli, 2001: Modification of an operational dispersion model for urban applications. *J. Applied Meteorol.*, **40**, 864-879.
- He, P., T. Katayama, T. Hayashi, J.-i. Tsutsumi, J. Tanimoto, and I. Hosooka, 1997: Numerical simulation of air flow in an urban area with regularly aligned blocks, *J. Wind Eng. & Ind. Aerodynam*, **67/68**, 281-291.
- Huang, H., R. Ooka, and S. Kato, 2005: Urban thermal environment measurements and numerical simulation for an actual complex urban area covering a large district heating and cooling system in summer, *Atmospheric Env.*, **39**, 6362-6375.
- Kunz, R.F., Venkateswaran, S., 2000: On the Roles of Implicitness, Realizability, Boundary Conditions and Artificial Dissipation in Multidimensional Two-Fluid Simulations with Interfacial Forces, AMIF-ESF Workshop on *Computing Methods for Two-Phase Flow*, Centre Paul Langevin, Aussois, France, 12-14.
- Kunz, R.F., Yu, W.S., Antal, S.P., Ettore, S.M., 2001: An Unstructured Two-fluid Method Based on the Coupled Phasic Exchange Algorithm, AIAA Paper 2001-2672.
- Kunz, R.F., Deutsch, S., Lindau, J.W., 2003: Two Fluid Modeling Of Microbubble Turbulent Drag Reduction, ASME Paper FED2003-45640, Proceedings of FEDSM'03: 4TH ASME-JSME Joint Fluids Engineering Conference, Honolulu, Hawaii, USA, July 6-11.
- Leung, M.K.H., C.-H. Liu, A.H.S. Chan, D.Y.C. Leung, W.C. Yam, S.P. Ng, and L.P. Vrigmoed, 2005: Prediction of transient turbulent dispersion by CFD-statistical hybrid modelling method, *Atmospheric Env.*, **39**, 6345-6351.
- Meng, J.C.S., Uhlman, J.S., 1998: Microbubble Formation and Splitting in a Turbulent Boundary Layer for Turbulence Reduction, *Proceedings of the International Symposium on Seawater Drag Reduction*, Newport, RI, 341-355.
- Moon, D. A. Albergel, F. Jasmin, and G. Thibaut, 1997: The use of the MERCURE CFD code to deal with an air pollution problem due to building wake effects, *J. Wind Eng. & Ind. Aerodynam*, **67/68**, 781-791.

Palmer, G., B. Vazquez, G. Knapp, N. Wright, 2005: The practical application of CFD to Wind engineering problems, Eighth International IBPSA Conference, Eindhoven, Netherlands.

Peltier, L.J., S.E. Haupt, R.F. Kunz, and J.J. Dreyer, 2005: Fine-Scale CFD of Building Flows with Diurnal Heating/Cooling, 9th Annual George Mason University Transport and Dispersion Modeling Conference, Fairfax, VA. July 18-20.

Pullen, J., Boris, J.P., Young, T., Patnaid, G. and Iseline, J., 2005: A comparison of contaminant plume statistics from a Gaussian puff and urban CFD model for two large cities, *Atmos. Env.*, 39, 1049-1068.

Thermoanalytics, 2005: RadTherm Technical Bulletins: 330: RadTherm transient CFD input. <http://www.thermoanalytics.com/support/bulletins/bulletin330/index.htm>. and 340: RadTherm's Convection Options. <http://www.thermoanalytics.com/support/bulletins/bulletin340/index.html>. (accessed 10/18/05)

Thilmany, J., 2005: Harms Way: Engineering software and microtechnology prepare

defense against bioterrorism, *Mechanical Engineering*, 127, 22-24.

NREL, 2005: Typical Meteorological Year Database (TMY2), [http://redc.nrel.gov/solar/old\\_data/nsrdb/tmy2/](http://redc.nrel.gov/solar/old_data/nsrdb/tmy2/) (accessed 4/20/05)

Van Doormal, J. P., Raithby, G. D., 1984: Enhancements of the SIMPLE Method for Predicting Incompressible Fluid Flows, *Numerical Heat Transfer*, 7, 147-163.

Warner, S. N. Platt, and J.F. Heagy, 2004: Comparisons of transport and dispersion model prediction of the URBAN 2000 Field experiment, *J. Applied Meteorol.*, 43, 829-846.

Wright, N.G. and G.J. Easom, 2003: Non-linear k- $\epsilon$  Turbulence Model Results for Flow Over a Building at Full-Scale, *Applied Mathematical Modelling*, 27, 1013-1033.

Yamada, T., 2005: Numerical simulations of air flows in and around a city in a coastal region, Proceedings of the Sixth Conference on Coastal Atmospheric and Oceanic Processes, San Diego, paper 5.6.